Supporting Information

Error compensated MOF-based ReRAM array for encrypted logical operations

Semyon V. Bachinin,[a] Sergey S. Rzjevskii,[a] Ivan Sergeev,[a] Svyatoslav A. Povarov,[a] Alena N. Kulakova,[a] Anastasia Lubimova,[a] Varvara Haritonova,[a] Valentine A. Milichko*[b]*

[a.] School of Physics and Engineering, ITMO University, Saint Petersburg, 197101, Russia
[b.] Institut Jean Lamour, Universit de Lorraine, UMR CNRS 7198, 54011, Nancy, France.
E-mail: semen.bachinin@metalab.ifmo.ru; valentin.milichko@univ-lorraine.fr

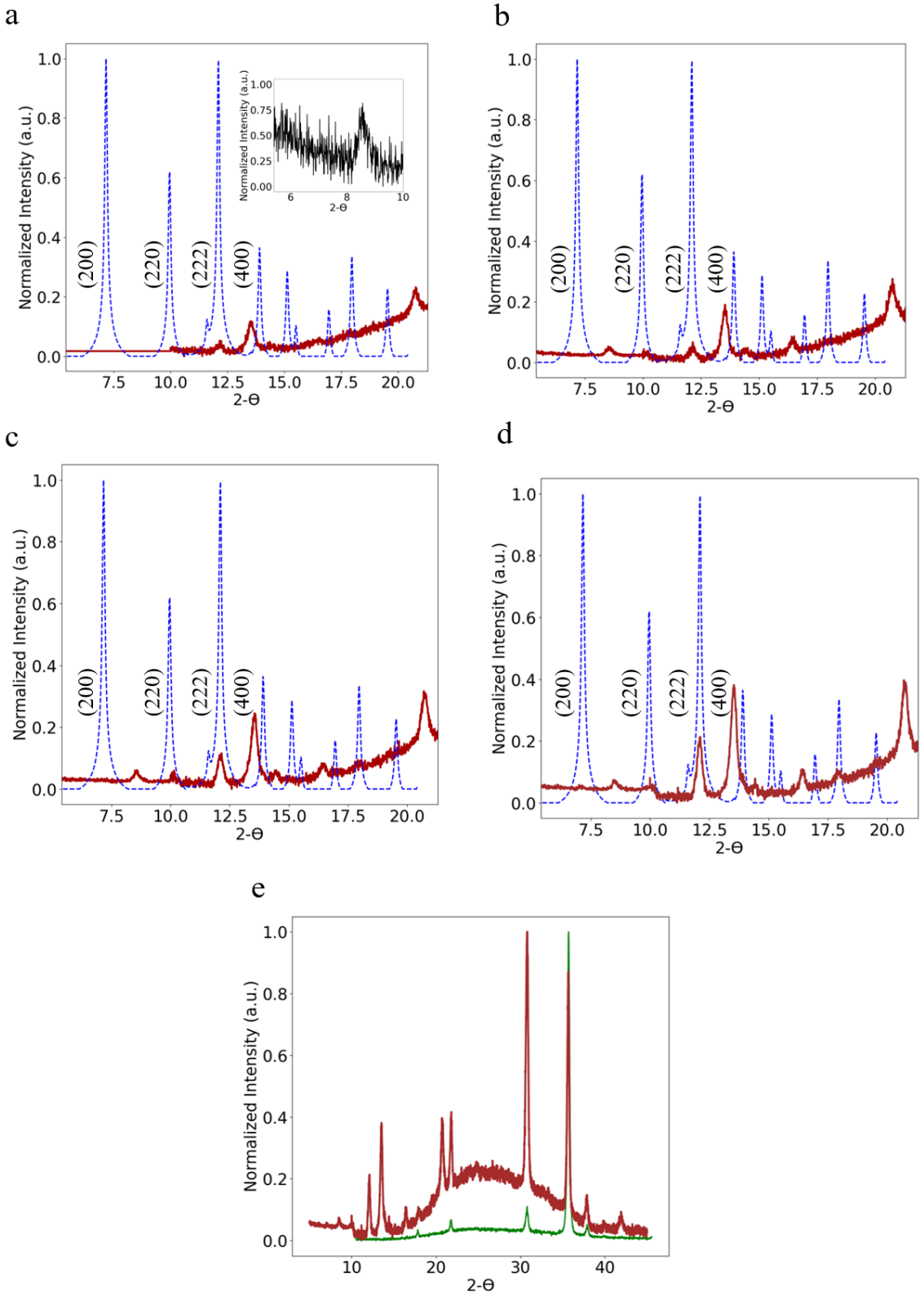

Figure S1. PXRD pattern of the HKUST-1 thin films (red curve) obtained on ITO (green curve in (e)) by different spin-coating cycles: a) 100 cycles, b) 200 cycles, c) 300 cycles, and d) 500 cycles. Model HKUST-1 is also represented (blue dotted curve, CCDC: 2091260). The HKUST-1 thin films revealed strong reflection peak at (400) plane, next to weaker reflection at (220) and (222) planes, corresponding tot he preferential orientation of HKUST-1 during the growth.

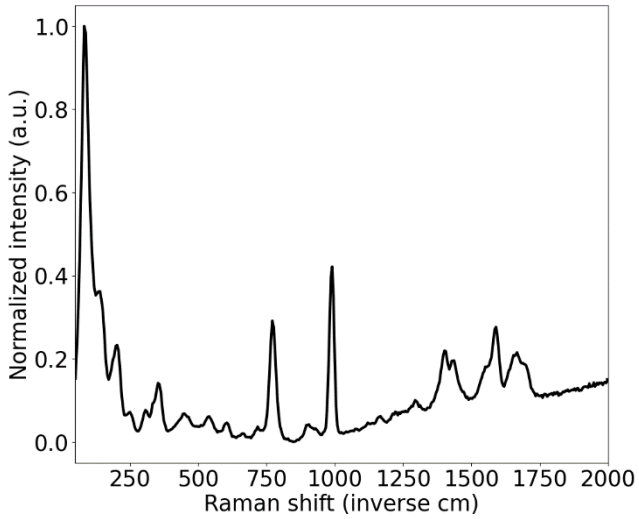

Figure S2. Raman spectra of the HKUST-1 thin film (150 nm thick).

Table S1. Interpretation of chemical bonds from Raman spectra of HKUST-1 thin film with the thickness of 150 nm.

Peak position, cm^{-1}	**Peak assignment**	**Ref.**
173	ν(Cu-Cu)	[13]
266	ν(Cu-Ow)	
495	ν(Cu-O)	
730,814	γ(C-H)	
929	ν(C-C)	
997,1610	ν(C=C)	
1430,1580	ν(COO)	

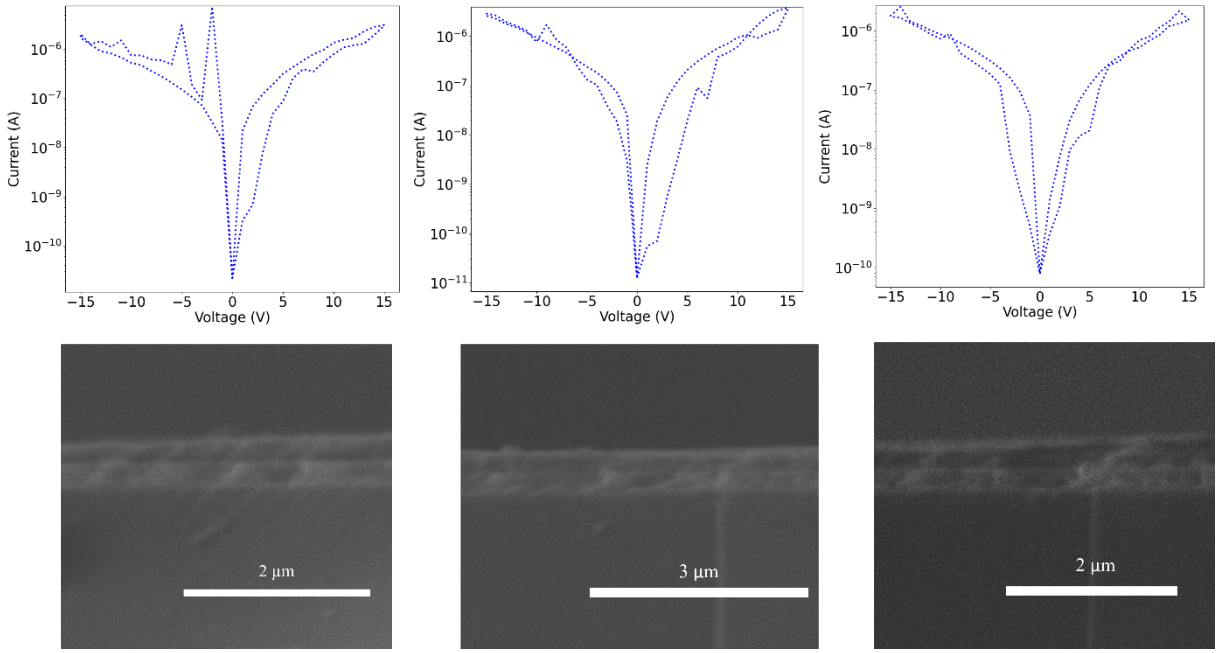

Figure S3. Current-voltage curves (top side) for the ReRAM cells and corresponding SEM cross-section micrographs (bottom side) for 200 spin-coating cycles HKUST-1 thin film.

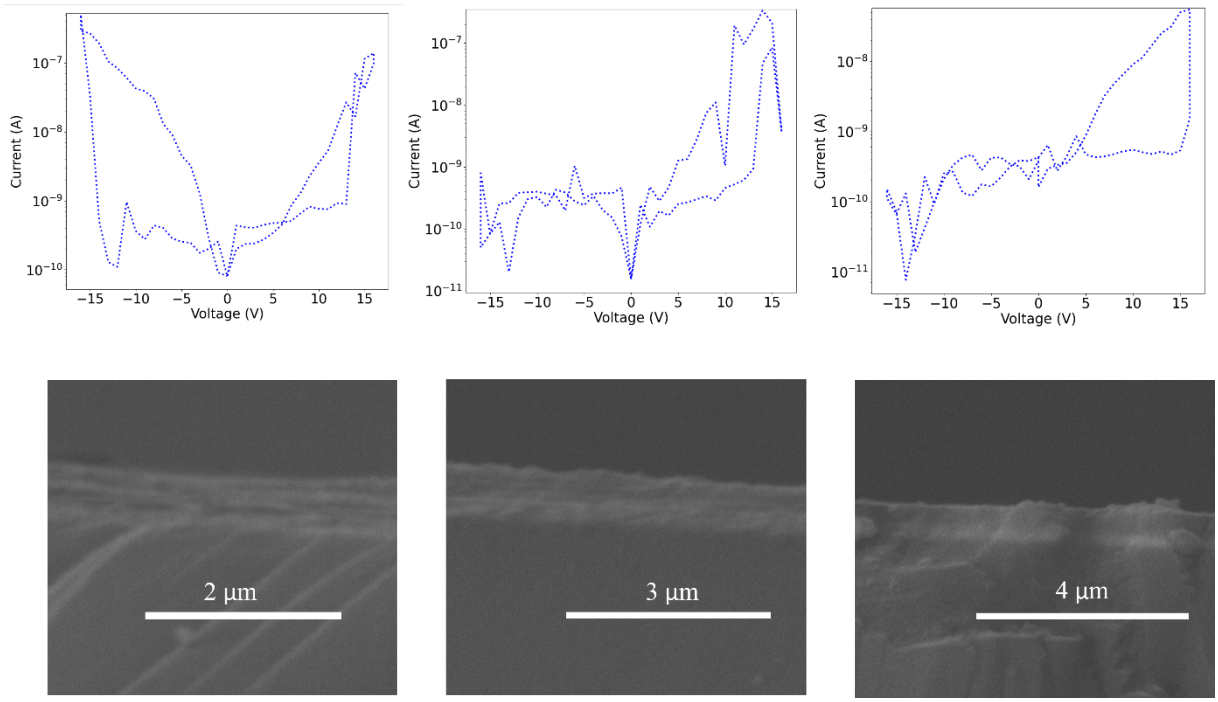

Figure S4. Current-voltage curves (top side) for the ReRAM cells and corresponding SEM cross-section micrographs (bottom side) for 300 spin-coating cycles HKUST-1 thin film.

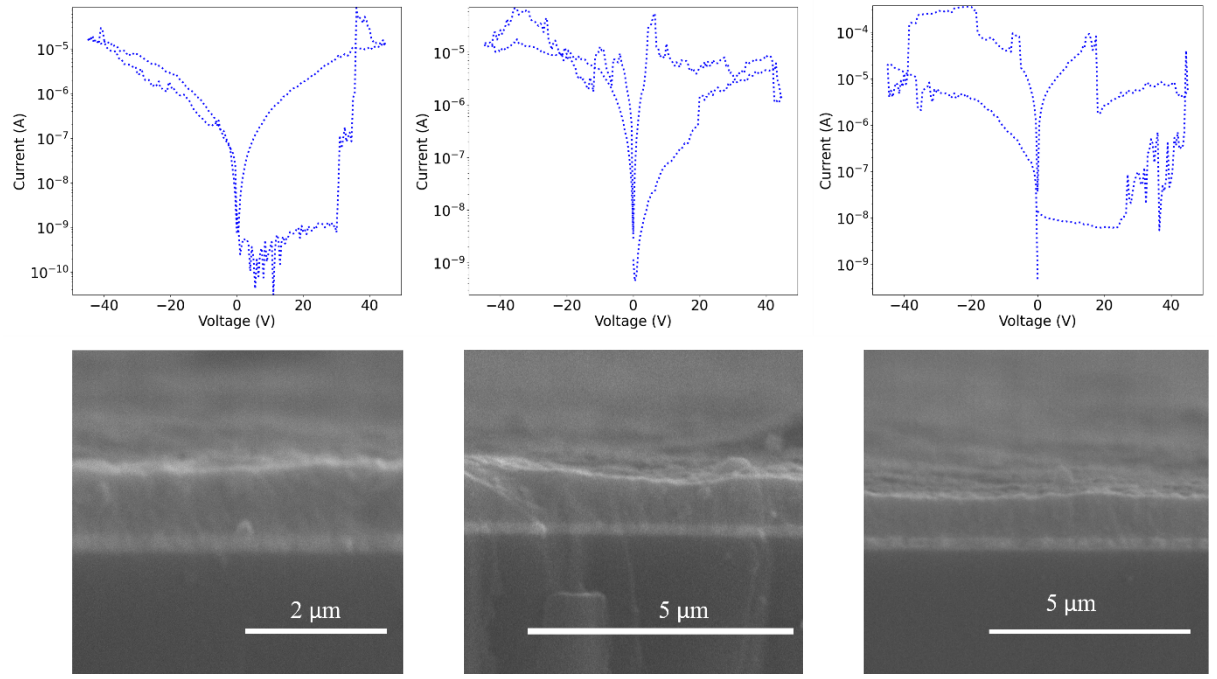

Figure S5. Current-voltage curves (top side) for the ReRAM cells and corresponding SEM cross-section micrographs (bottom side) for 500 spin-coating cycles HKUST-1 thin film.

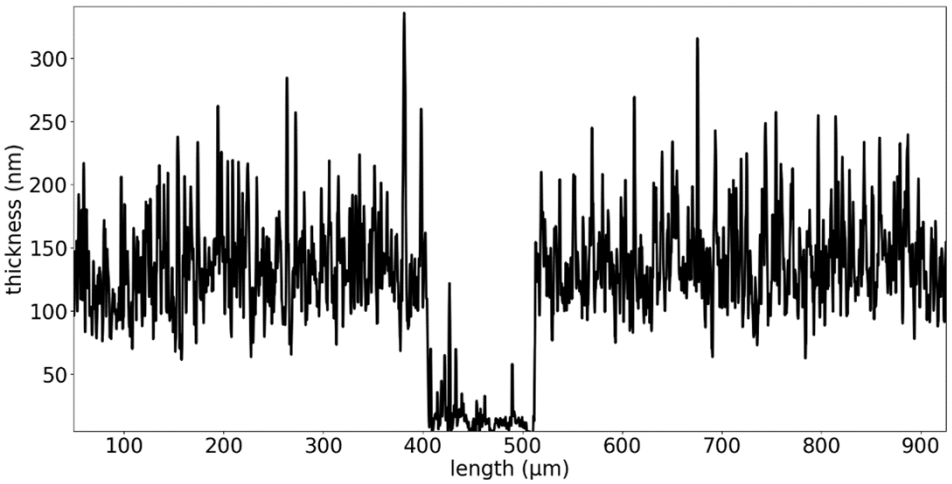

Figure S6. Ellipsometry of 100 spin-coating cycles HKUST-1 thin film.

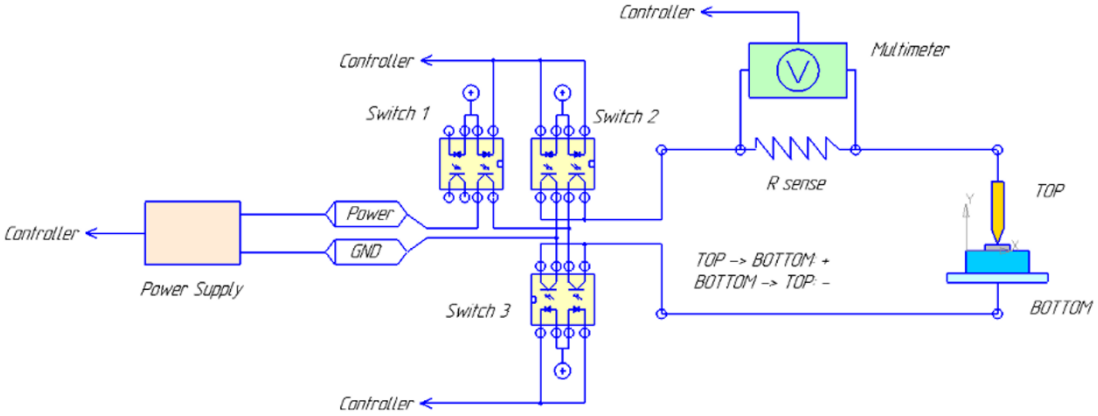

Figure S7. Electrical scheme for current-voltage measurements.

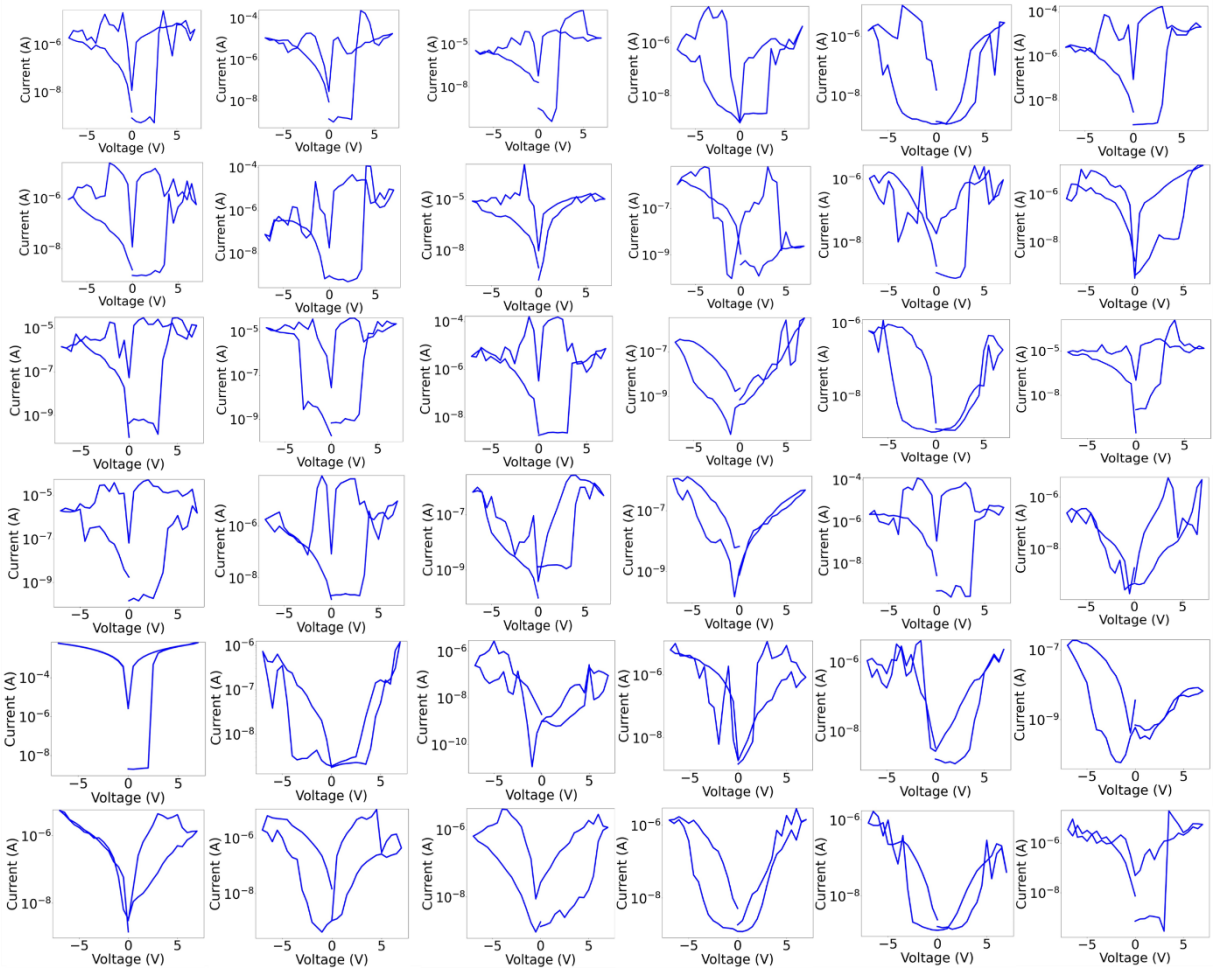

Figure S8. The set of current-voltage curves for 6x6 ReRAM cells of the prototype from Figure 1a.

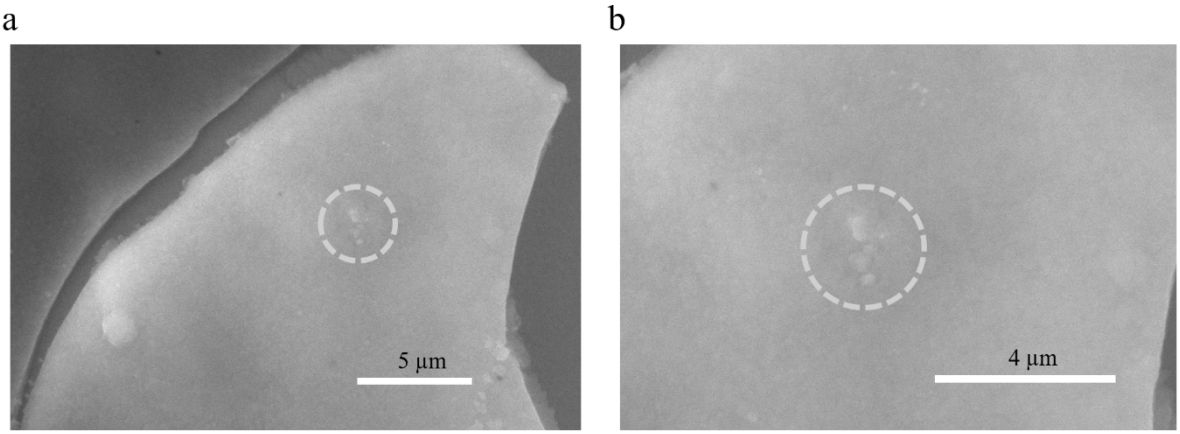

Figure S9. (a,b) SEM micrographs of the HKUST-1 film surface area where the stability of memristive behavior (in 50 set/reset cycles) was studied.

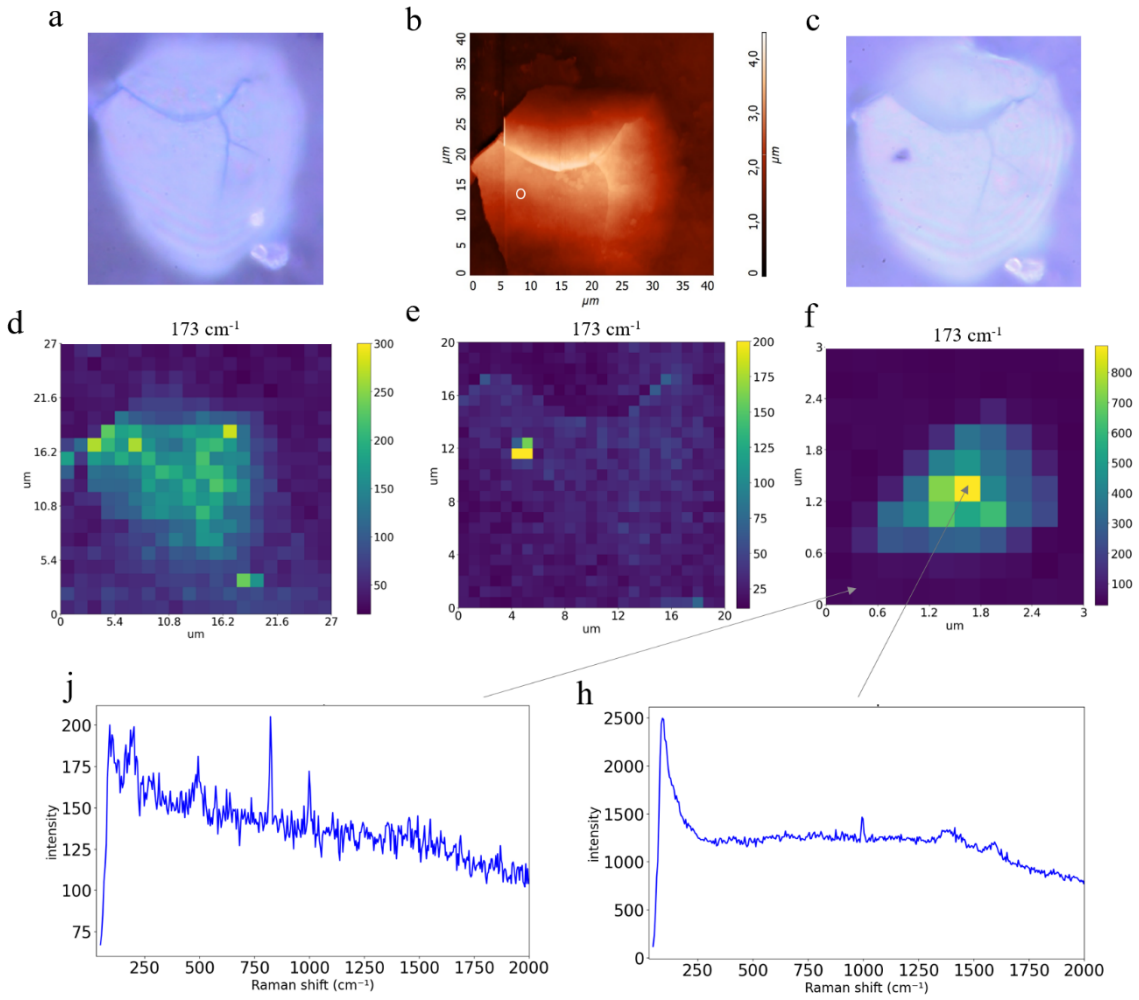

Figure S10. (a) Optical image of the HKUST-1 film surface area before the applied voltage. (b) Atomic force microscopy image of the same area (circled) before the applied voltage. (c) Optical image of the HKUST-1 film surface area after the applied voltage (4 V). (d) Raman spectroscopy map of the intensity distribution of the ν(Cu-Cu) bond (173 cm^{-1}) of the HKUST-1 film surface area before the applied voltage. (e,f) Raman spectroscopy map of the intensity distribution of the ν(Cu-Cu) bond of the HKUST-1 film surface area after the applied voltage (4 V). (j) Raman spectra over different areas of the HKUST-1 film after the applied voltage.

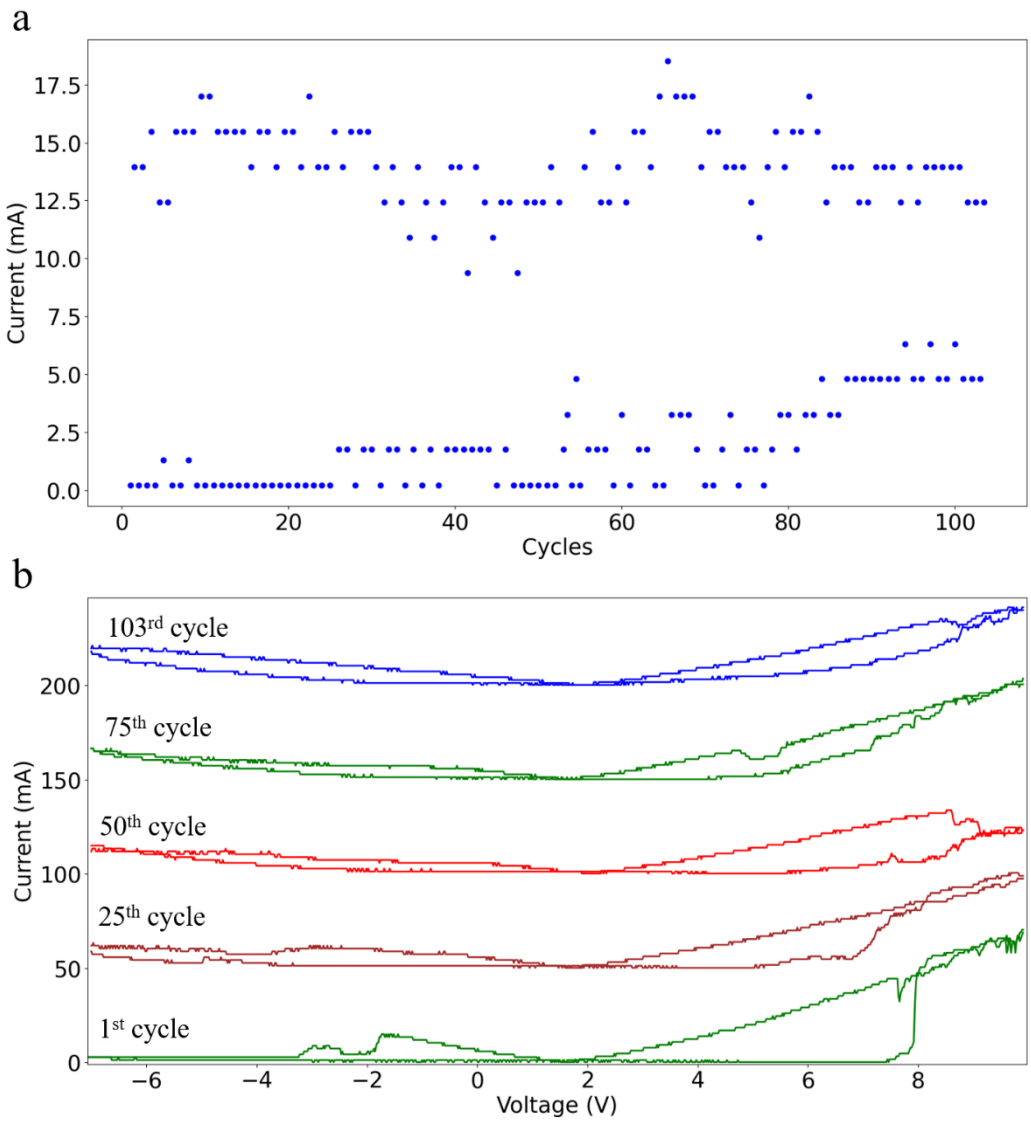

Figure S11. (a) Endurance (set/reset cycles) of the HKUST-1 film, analyzed by the current atomic force microscopy (reading voltage was 4 V). (b) Volt-Ampere characteristic curves.

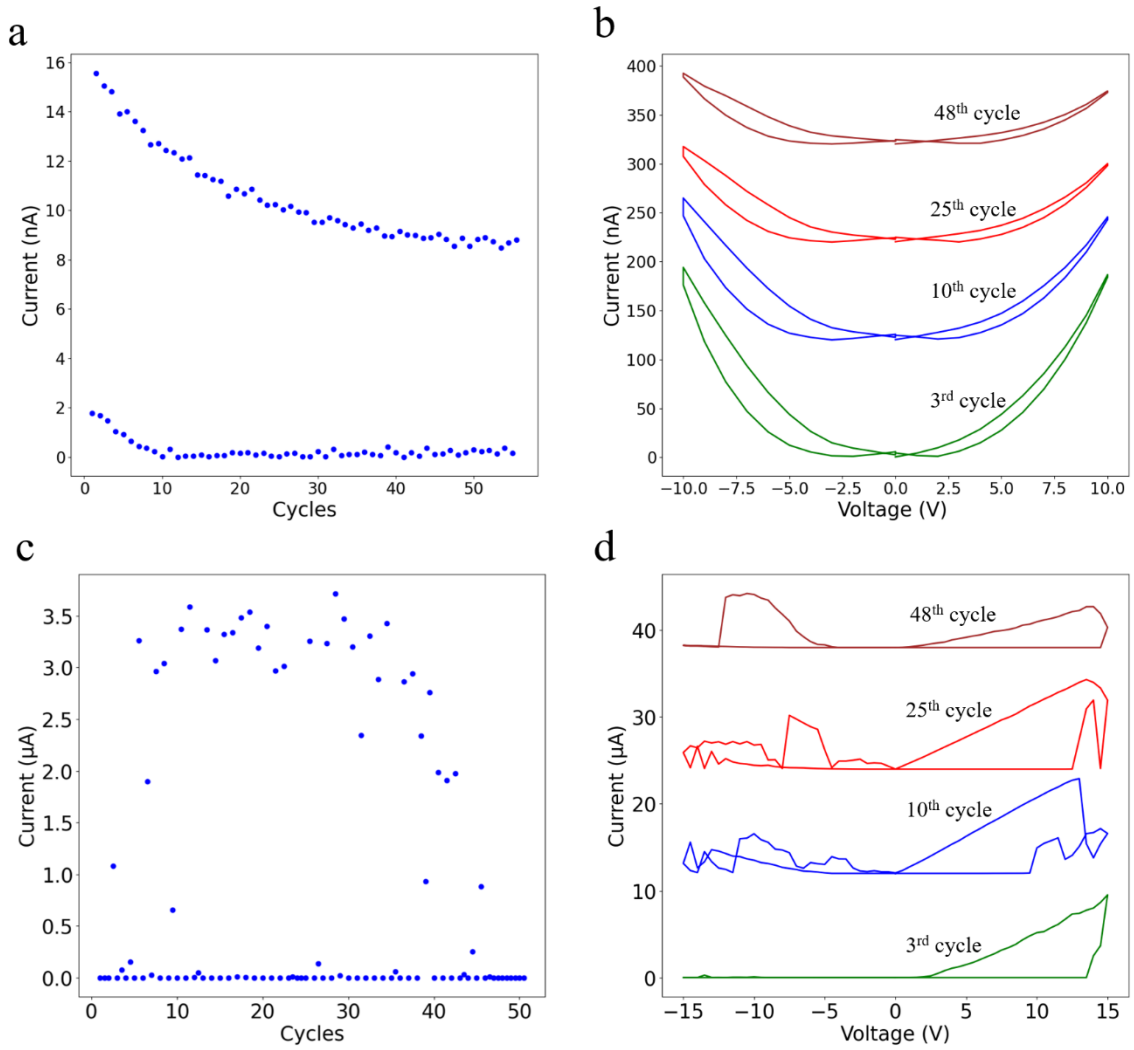

Figure S12. Comparison of the endurance for the same ReRAM cell after 2 years of storage under normal conditions. (a,b) Initial cell, and (c,d) the cell after 2 years of storage.

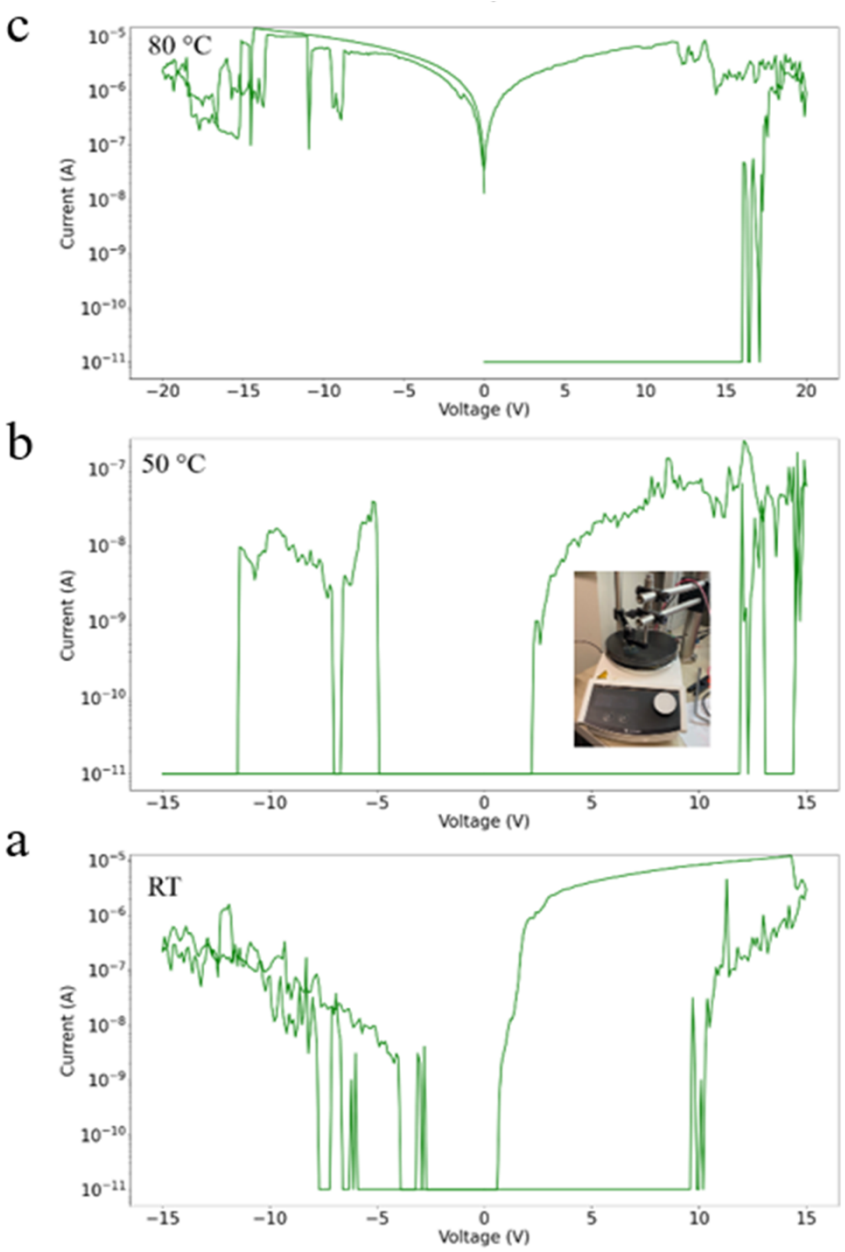

Figure S13. An effect of heat on the operation parameters of ReRAM cell, measured at room temperature (a), at 50 °C (b), and 80 °C (c).

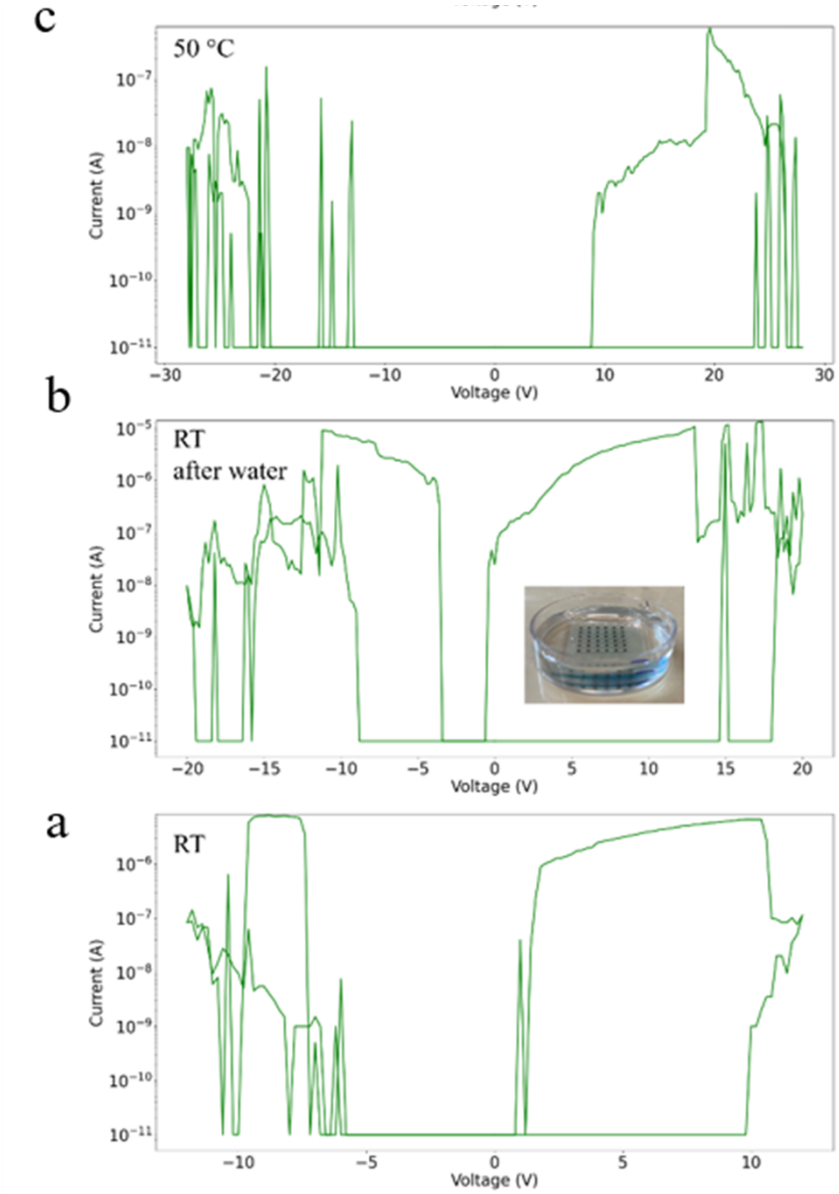

Figure S14. An effect of heat and water on the operation parameters of the ReRAM cell, measured at room temperature (a), after immersion in water for 1 min and drying at room temperature (b), and after heating the same cell up to 50 °C (c).

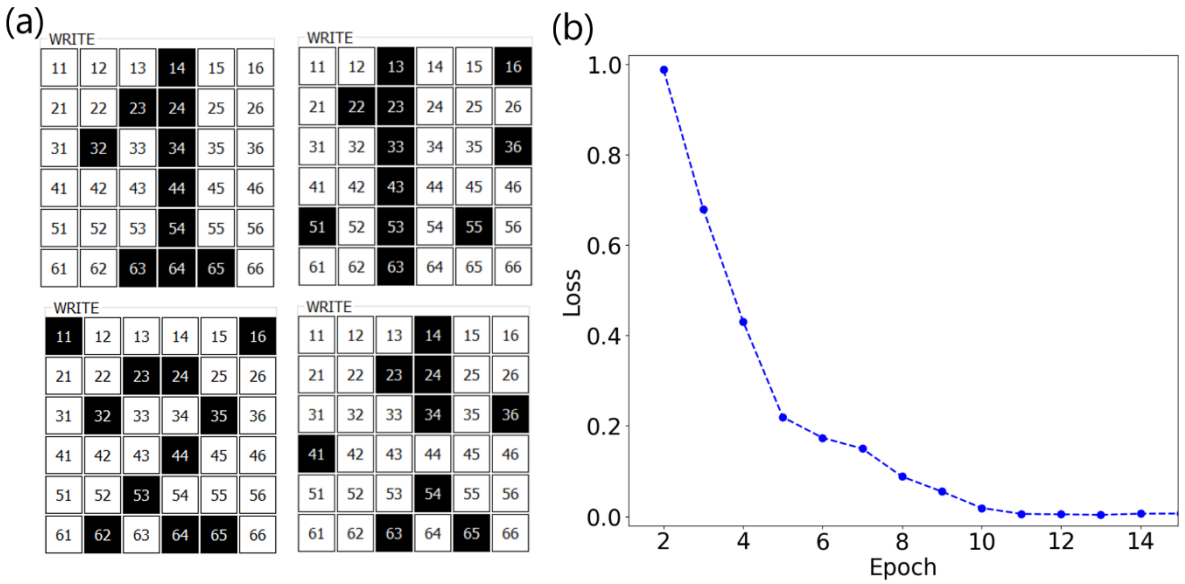

Figure S15. (a) Different results of reading from our prototype. (b) Error compensation for reading the information via neural network.

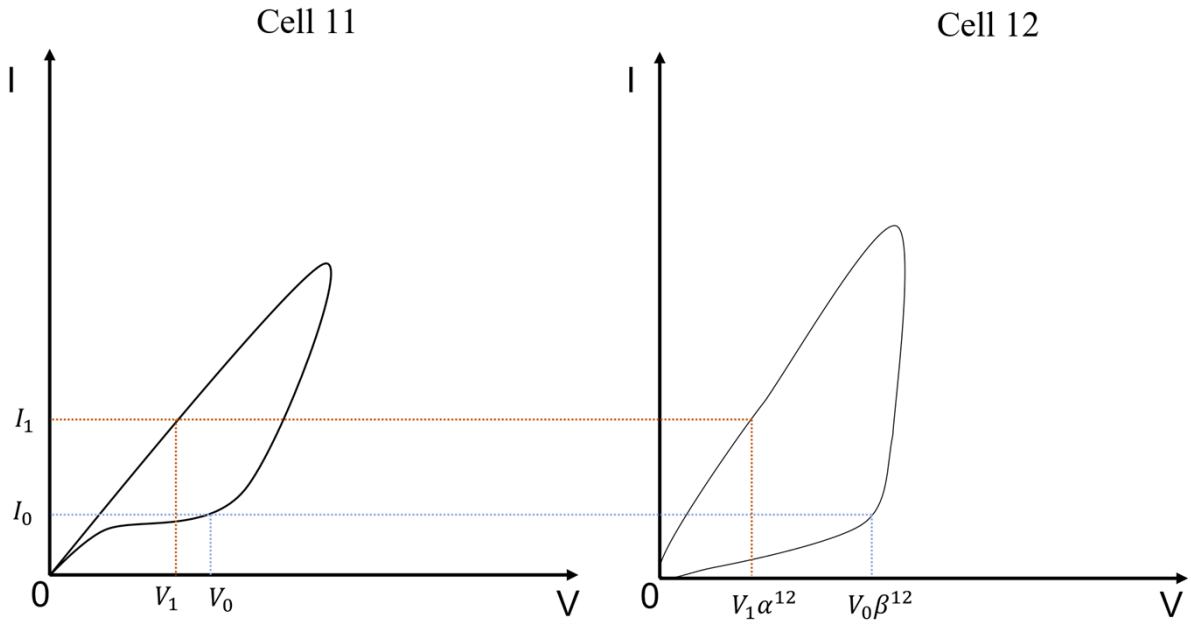

Figure S16. The schematic current-voltage curves (see Figure S8) for different ReRAM cells (11 and 12), allowing one to determine the coefficients (α^{12}, β^{12}) at a specific applied voltage V_1 and V_0.

Table S2. Correspondence of the resulting current to the numerical result (in Figure 3c).

Number, *N*	**Current (μA)**
0	7.876327
1	13.485707
2	19.095087
3	24.704467

4	30.313846
5	35.923226
6	41.532606
7	47.141986
8	52.751365
9	58.360745
10	63.970125
11	69.579505
12	75.188884
13	80.798264
14	86.407644
15	92.017024
16	97.626403
17	103.235783
18	108.845163
19	114.454543
20	120.063922
21	125.673302
22	131.282682
23	136.892062
24	142.501441
25	148.110821
26	153.720201
27	159.329581
28	164.93896
29	170.54834
30	176.15772

Symbol encryption (via ASCII strategy):

M —ASCII→ 77 → [(77 * 0.974)] → 75 —ASCII→ K
O —ASCII→ 79 → [(79 * 0.517)] → 41 —ASCII→)
F —ASCII→ 70 → [(70 * 0.899)] → 63 —ASCII→ ?

To decrypt, we perform the reverse process:
K —ASCII→ 75 → [(75 / 0.974)] → 77 —(ASCII)→ M
) —ASCII→ 41 → [(41 / 0.517)] → 79 —(ASCII)→ O
? —ASCII→ 63 → [(63 / 0.899)] → 70 —(ASCII)→ F